REPORT

CRB2 Mutations Produce a Phenotype Resembling Congenital Nephrosis, Finnish Type, with Cerebral Ventriculomegaly and Raised Alpha-Fetoprotein

Anne Slavotinek,[1,2,*] Julie Kaylor,[3] Heather Pierce,[4] Michelle Cahr,[5] Stephanie J. DeWard,[4] Dina Schneidman-Duhovny,[6,7] Adnan Alsadah,[1] Fadi Salem,[8] Gabriela Schmajuk,[9] and Lakshmi Mehta[5]

We report five fetuses and a child from three families who shared a phenotype comprising cerebral ventriculomegaly and echogenic kidneys with histopathological findings of congenital nephrosis. The presenting features were greatly elevated maternal serum alpha-fetoprotein (MSAFP) or amniotic fluid alpha-fetoprotein (AFAFP) levels or abnormalities visualized on ultrasound scan during the second trimester of pregnancy. Exome sequencing revealed deleterious sequence variants in Crumbs, *Drosophila*, Homolog of, 2 (*CRB2*) consistent with autosomal-recessive inheritance. Two fetuses with cerebral ventriculomegaly and renal microcysts were compound heterozygotes for p.Asn800Lys and p.Trp759Ter, one fetus with renal microcysts was a compound heterozygote for p.Glu643Ala and p.Asn800Lys, and one child with cerebral ventriculomegaly, periventricular heterotopias, echogenic kidneys, and renal failure was homozygous for p.Arg633Trp in *CRB2*. Examination of the kidneys in one fetus showed tubular cysts at the corticomedullary junction and diffuse effacement of the epithelial foot processes and microvillous transformation of the renal podocytes, findings that were similar to those reported in congenital nephrotic syndrome, Finnish type, that is caused by mutations in nephrin (*NPHS1*). Loss of function for *crb2b* and *nphs1* in *Danio rerio* were previously shown to result in loss of the slit diaphragms of the podocytes, leading to the hypothesis that nephrosis develops from an inability to develop a functional glomerular barrier. We conclude that the phenotype associated with *CRB2* mutations is pleiotropic and that the condition is an important consideration in the evaluation of high MSAFP/AFAFP where a renal cause is suspected.

The family of Crumbs proteins, homologous to *Drosophila* Crumbs (Crb), contain large extracellular domains with epidermal growth factor (EGF)-like repeats and laminin-globular domains, a single transmembrane domain, and a short, intracellular C terminus containing single FERM and PDZ protein-binding motifs.[1,2] In *D. melanogaster*, Crb is expressed in ectoderm and on the apical membranes of epithelial cells.[3,4] Aberrant Crb function disrupts the organization of epithelia derived from ectoderm during organogenesis and the maintenance of epithelial cell polarity.[3,5] The PDZ-binding motif can recruit a plasma membrane-associated protein scaffold comprising Stardust (Sdt), DPatJ and DLin7 or Partitioning-defective protein 6 (Par6), and atypical protein kinase C (aPKC) to form the Crumbs complex.[6] Studies in *D. melanogaster* and *D. rerio* show that the Crumbs complex can regulate cellular signaling pathways, such as Notch, Homolog of, 1 (Notch1), mechanistic target of rapamycin complex 1 (mTORC1), and the Hippo pathway.[6–9]

There are three Crb genes in humans: Crumbs homolog-1 (*CRB1* [MIM 604210]), Crumbs homolog-2 (*CRB2* [MIM 609720]), and Crumbs homolog-3 (*CRB3* [MIM 609737]).[10] In humans, mutations in *CRB1* cause a spectrum of eye defects, including progressive retinitis pigmentosa (RP12 [MIM 600105]) accompanied by retinal thickening and an absence of distinct retinal layers, RP with Coats-like exudative vasculopathy, Leber's congenital amaurosis (LCA8 [MIM 613835]),[11–13] childhood cone-rod dystrophy and macular cystic degeneration,[14] and macular dystrophy.[15] The association of eye defects with loss of *CRB1* function is supported by studies showing that ablation of *Cbr1* and *Crb2* in the murine retina leads to defects in lamination and proliferation of retinal progenitor cells that is similar to LCA, with dysregulation of the Notch1 and YAP/Hippo signaling pathways involved in cell proliferation.[9] Although *CRB1* expression is strongest in the retina and brain, it is also detectable in the kidney, skin, lung, and colon,[16,17] but we could find no reports of extra-ocular manifestations in individuals with *CRB1* mutations.

Less is known about the clinical findings resulting from mutations in *CRB2*. This gene has 13 exons and encodes a 1,285 amino acid transmembrane protein that is predominantly expressed in human fetal eye, retinal pigment epithelium/choroid, brain, and kidney, with weaker expression in the heart, placenta, and lung.[18] Mutation analysis of *CRB2* in 85 persons with RP and 79 persons with LCA revealed 11 missense substitutions, but no individual had two mutations compatible with

[1]Department of Pediatrics, Division of Genetics, University of California, San Francisco, San Francisco, CA 94143-2711, USA; [2]Institute for Human Genetics, University of California, San Francisco, 513 Parnassus Avenue, San Francisco, CA 94143-0794, USA; [3]Molecular Genetics Pathology Laboratory, Arkansas Children's Hospital, 1 Children's Way, Slot 820, Little Rock, AR 72202, USA; [4]GeneDx, Inc., 207 Perry Parkway, Gaithersburg, MD 20877, USA; [5]Division of Medical Genetics, Icahn School of Medicine at Mount Sinai & Mount Sinai Medical Center, 1 Gustave Levy Place, New York, NY 10029, USA; [6]Department of Bioengineering and Therapeutic Sciences, University of California, San Francisco, San Francisco, CA 94158, USA; [7]Department of Pharmaceutical Chemistry, University of California, San Francisco, San Francisco, CA 94158, USA; [8]Department of Pathology, Icahn School of Medicine at Mount Sinai & Mount Sinai Medical Center, 1 Gustave Levy Place, New York, NY 10029, USA; [9]Division of Rheumatology, Department of Medicine, UCSF and the San Francisco VA Hospital, 4150 Clement St, Mailstop 111R, San Francisco, CA 94121, USA
*Correspondence: slavotia@ucsf.edu
http://dx.doi.org/10.1016/j.ajhg.2014.11.013.

Table 1. Clinical Features Associated with *CRB2* Mutations in Cases from Three Families

	Family 1 (Sib 1)	Family 1 (Sib 2)	Family 2 (Sib 1)	Family 2 (Sib 2/ Twin A)	Family 2 (Sib 3)	Family 3
Age at diagnosis	18 weeks gestation	17 weeks gestation	17 weeks gestation	16 weeks gestation	16 weeks gestation	20 weeks gestation
Central Nervous System						
Ventriculomegaly	+; 15 mm	+; 13 mm	+; 14 mm			+; 12–16 mm
Grey matter heterotopias						+
Cardiac						
Ventricular septal defect						+
Pericardial effusion		+ (US)				
Renal						
Renal echogenicity		+ (US)				+ (US)
Microcysts	+	+	+		+	
Outcome	TOP	TOP	TOP	TOP	TOP	expired at 7 months
Amniotic Fluid Testing						
MSAFP	18 MoM	8 MoM	13 MoM	5 MoM (twins)	9 MoM	not done
AFAFP	45 MoM	89 MoM	25 MoM	24 MoM	18 MoM	not done
AF acetylcholinestrase	wk + ve	wk + ve	wk + ve	wk + ve	negative	not done
Investigations						
Karyotype	46,XX	46,XY	46,XX	46,XY	46,XY	
Array CGH	Arr(1-22)x2	Arr(1-22)x2		Arr(1-22)x2	Arr(1-22)x2	Arr(1-22)x2
NPHS1 sequencing				no mutations		c.1440+1G>A
CRB2 sequencing	p.Trp759Ter/ p.Asn800Lys	p.Trp759Ter/ p.Asn800Lys	not done	not done	p.Glu643Ala/ p.Asn800Lys	p.Arg633Trp/ p.Arg633Trp

Abbreviations are as follows: AF acetylcholinestrase, amniotic fluid acetylcholinesterase; AFAFP, amniotic fluid alpha-fetoprotein; Array CGH, array comparative genomic hybridization; MoM, multiple of median; MSAFP, maternal serum alpha-fetoprotein; TOP, termination of pregnancy; US, ultrasound scan finding; wk + ve, weakly positive.

autosomal-recessive inheritance of *CRB2* sequence variants as a cause of their disease.[18] Conditional null mice that lack *Crb2* in the developing retina showed progressive thinning and degeneration of the photoreceptor layer, with abnormal lamination of immature rod photoreceptors and disruption of the adherens junctions between photoreceptors, Müller glia, and progenitor cells.[7] The retinal degeneration was severe and mimicked the RP caused by mutations in *CRB1* in humans.[10] Complete loss of *Crb2* in mice led to developmental anomalies beginning at gastrulation and embryonic lethality by embryonic day (E) 12.5.[19] In the absence of *Crb2*, the head fold, heart tube, foregut invagination, and somite development were all disturbed; heterozygotes were viable, fertile, and without abnormalities.[19] This suggests that abnormal *Crb2* function might be associated with a broader phenotype that includes multiple malformations and lethality. We present three families with *CRB2* mutations inherited as an autosomal-recessive trait that were detected on whole exome sequencing, documenting a consistent phenotype that includes cerebral, renal, and cardiac malformations.

A summary of the clinical findings is provided in Table 1. In the first family, both parents were nonconsanguineous and were of Austrian, German, Scottish, and Ashkenazi Jewish ethnicity. In her second pregnancy, the mother was 34 years of age and G2P1. An ultrasound (US) scan at 18 weeks of gestation showed severe cerebral ventriculomegaly measuring 15 mm, midface hypoplasia, a single umbilical artery, and a small stomach and bladder. The maternal serum (MS) alpha-fetoprotein (AFP) was 18 multiple of median (MoM). Amniocentesis revealed an amniotic fluid (AF) AFP of 45 MoM with a weakly positive acetylcholinesterase. Chromosome analysis showed a normal female karyotype and array comparative genomic hybridization (array CGH; Clarisure Oligonucleotide-SNP array with 2.67 million probes and 1.15 kb resolution) did not detect any abnormalities. The couple opted not to continue the pregnancy. At a limited autopsy performed at 19 weeks gestation, foot length was 2.9 cm (expected 3.3 ± 0.6 cm). The heart weighed 1.3 g (expected 2.9 g), and the left and right kidneys each weighed 1.0 g (combined weight 2.0 g; expected 2.9 g). The renal cortex was normal for gestational age, but there were numerous, greatly dilated tubules and microscopic cysts in the renal medulla. The heart was normal on examination and the brain and spinal cord were unable to be assessed.

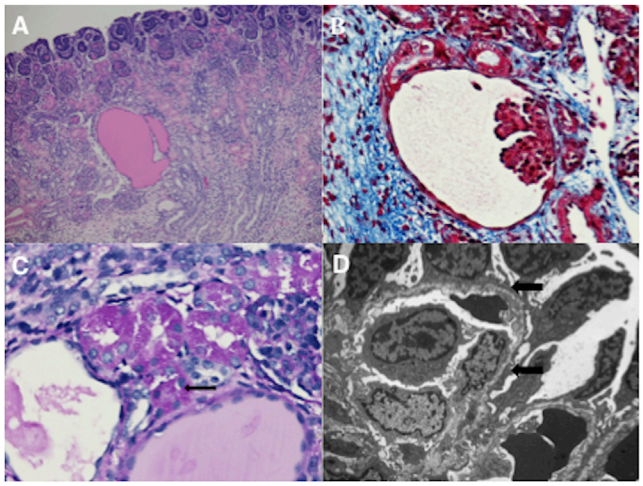

Figure 1. Renal Findings Associated with Compound Heterozygosity for p.Glu743Ala and p.Asn800Lys Mutations in *CRB2*
(A) Low-power view of the kidney shows focal tubular cyst at the corticomedullary junction. Cyst is filled with eosinophilic material. Normal-appearing glomeruli are seen in the cortex (hematoxylin and eosin ×10).
(B) An infantile glomerulus with dilatation of Bowman's space forms a glomerular microcyst (Masson trichrome stain ×40).
(C) Proximal tubular epithelial cells contain numerous protein resorption droplets (arrow). Below the tubules, microcysts with attenuated lining are seen (periodic acid-Schiff ×60).
(D) Glomerulus shows crowding and hypertrophy of the podocytes, and complete effacement of foot processes (arrows) with focal microvillous transformation (transmission electron microscope ×2,500).

In the next pregnancy, the mother was 36 years of age and G3P1TAB1. An US scan at 12 weeks was reported as normal. AFAFP was elevated at 88.92 MoM and AF acetylcholinesterase was again weakly positive, but with negative hemoglobin F. Array CGH showed a normal male karyotype. A repeat US scan at 17 weeks 5 days of gestation showed a head circumference of 14.87 cm (consistent with 18 weeks 0 days), foot length of 2.28 cm (16 weeks 6 days), and the estimated fetal weight was 190 g. Significant ventriculomegaly was again noted and the diameter of the atrium of the lateral ventricles measured 13 mm. The cerebellum was described as asymmetric. The anterior portion of the corpus callosum was developed, but the posterior part was not definitely visualized and this was attributed to early gestational age. A large pericardial effusion, echogenic changes in the right ventricular myocardium, and a suspected ventricular septal defect (VSD) were also observed. The fetal kidneys were slightly enlarged and echogenic and the fetal bowel was also echogenic. The umbilical cord had three vessels. A diagnosis of Finnish nephrosis was proposed and the couple opted not to continue with the pregnancy. At autopsy, foot length was 2.8 cm (expected 2.8 cm). A limited examination showed a structurally normal heart with no VSD. Only one globular kidney was identified that measured 0.5 cm and weighed 0.5 g (expected weight 1.1 g). Histology of the kidney showed normal glomeruli, but the medullary architecture was abnormal, with microscopic medullary cysts and clusters of distal tubules dispersed randomly between the glomeruli.

In the second family, the nonconsanguineous parents were healthy and of Ashkenazi and Ashkenazi/Sephardic Jewish ethnicity. The mother was 30 years old and G2P1 at the time of the first affected pregnancy. The MSAFP was 13 MoM at 17 weeks gestation and a fetal US at 17 weeks 4 days gestation showed hydrocephalus, with lateral ventricles measuring 14 mm and dilatation of the third ventricle. Amniocentesis showed an AFAFP of 25.49 MoM, weakly positive acetyl-cholinesterase, and normal female chromosomes. The pregnancy was terminated at 19 weeks gestation. Pathology revealed scattered renal tubular cysts that were lined by attenuated epithelium and contained colloid-like content, consistent with congenital nephrosis. The proximal tubules contained intracytoplasmic eosinophilic droplets within the epithelial cells and there were no obvious glomerular findings. The brain was unable to be examined.

In the next affected pregnancy to the 31-year-old, G4P1TAB1 mother, the fetus was a twin from a spontaneously conceived dichorionic, diamniotic twin pregnancy. The MSAFP was 5 MoM and an amniocentesis performed at 16 weeks of gestation showed fetus A (male) had an AFAFP of 23.66 MoM with a faint acetylcholinesterase band. Fetus B (female) had normal AFAFP and both fetuses had a normal karyotype. An US was reported as normal at the time of amniocentesis, with lateral ventricles measuring 6 mm in fetus A. An oligonucleotide (44k) microarray, sequencing of nephrin *NPHS1* (MIM 602716) for congenital nephrotic syndrome, Finnish type (MIM 256300; also known as congenital nephrosis, Finnish type), and sequencing of solute carrier family 17 member 5 (*SLC17A5* [MIM 604322]) for infantile sialic acid storage disease (MIM 269920) were unremarkable in fetus A. The parents elected to selectively terminate the affected fetus.

The mother had a third affected pregnancy when she was 34 years of age and G5P2TAB2. MSAFP performed prior to amniocentesis at 16 weeks gestation was 9.24 MoM. AFAFP was 17.9 MoM and acetylcholinesterase was negative. An US scan was normal at the time of amniocentesis. The couple chose to terminate the pregnancy. At autopsy, the kidney showed scattered, tubular cysts at the corticomedullary junction that were lined by flattened epithelial cells and filled with glassy eosinophilic material (Figure 1A). There was focal mild dilatation of subcapsular glomerular Bowman's capsules (Figure 1B). Many proximal tubular epithelial cells contained intracytoplasmic eosiniophilic droplets consistent with protein on trichrome, periodic acid Schiff (PAS), and Jones stains (Figure 1C). Electron microscopy showed diffuse effacement of the epithelial foot processes and microvillous transformation of the podocytes, compatible with congenital nephrosis, Finnish type (Figure 1D). Examination of the brain was normal, with primitive neuroblast-like cells in the cortex. There was slight-to-moderate microglial activation in the

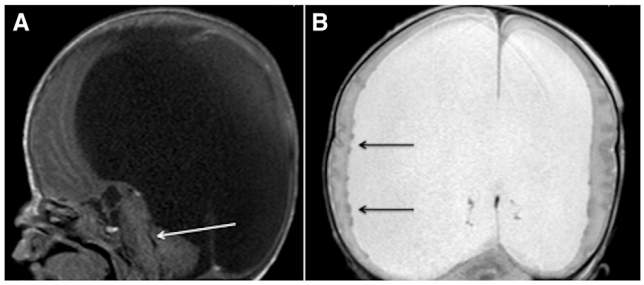

Figure 2. Hydrocephalus and Subependymal Grey Matter Heterotopias Associated with Homozygosity for p.Arg633Trp in CRB2

(A) Sagittal section of MRI scan of the brain at 1 day of age. There is severe hydrocephalus of the lateral ventricles, with compression of the brainstem and cerebellum. The arrow shows the compressed fourth ventricle.

(B) Coronal section of MRI scan of the brain at 1 day of age. There are numerous subependymal gray matter heterotopias, indicated by the arrows.

white matter, and migrating neurons from the germinating matrix were observed without any identifiable abnormalities.

In the third family, the male proband was born at 35 weeks to a 21-year-old, G3P2A1 mother and her nonconsanguineous partner. A 20 week US revealed bilateral ventriculomegaly, with the right ventricle measuring 12.6 mm and the left ventricle measuring 16.1 mm, nuchal fold thickening at 9.5 mm, an echogenic intracardiac focus within the left ventricle, and echogenicity of the bowel and kidneys. A fetal echocardiogram revealed normal cardiac segmentation, a mildly dilated ascending aorta (Z score = 3), and a small, perimembranous VSD. An US scan at 33 weeks gestation revealed an appropriate abdominal circumference for dates, but the fetal head measured 4 weeks larger than expected and the cerebral ventriculomegaly had increased to almost 3 cm bilaterally. The femurs were short ($<10^{th}$ percentile). The kidneys were mildly enlarged and demonstrated significant echogenicity. Fetal MRI was performed and revealed marked dilation of the lateral and third ventricles. There was nodularity along the lateral border of the left lateral ventricle suggestive of gray matter heterotopias. On the final US prior to delivery at approximately 33 weeks gestation, the right and left ventricles measured 5.7 cm and 3.7 cm, respectively.

The baby was delivered at 35 weeks with a birth weight of 3,950 g ($>97^{th}$ centile) and length 45 cm (25^{th} centile). APGAR scores were 2 at 1 min and 7 at 5 min. A brain MRI scan performed after birth showed massive ventriculomegaly involving the lateral and third ventricles with innumerable, subependymal gray matter heterotopias (Figure 2). A ventriculoperitoneal shunt was placed on the second day of life. A prolonged, continuous video electroencephalogram (EEG) was abnormal, with a discontinuous background pattern with multifocal spikes and severe episodes of myoclonic jerking. A seizure with right hand elevation and rhythmic eye blinking was noted with an ictal onset from the right frontoparietal region. Repeat video EEGs were also abnormal, with asymmetric background frequencies over the hemispheres and rhythmic, left-sided seizure activity during a cyanotic event. His seizures were later controlled with three antiepileptic drugs.

The initial postnatal renal US revealed enlargement of both kidneys to the upper limits of normal, with echogenicity and poor cortico-medullary differentiation. A repeat renal US at 23 days of life demonstrated kidney sizes at the upper limits of normal to mildly enlarged, with persistent echogenicity and grade 1 hydronephrosis. At 1 month 17 days, he developed edema of the scrotum and lower extremities. He had proteinuria that did not respond to combination therapy of angiotensin-converting-enzyme inhibitors and nonsteroidal anti-inflammatory drugs and he remained dependent on albumin infusions to maintain a stable weight. His last renal US continued to show diffusely echogenic kidneys with ascites. A SNP microarray (CytoScan HD, Affymetrix) was normal. The family deferred a renal biopsy and the child was discharged to palliative care at 6 months of age and was deceased at 7 months of age.

Whole exome sequencing (WES; GeneDx) was performed on exon targets isolated by capture with the Agilent SureSelect Human All Exon V4 (50 Mb) kit (Agilent Technologies). For the three trios comprising both parents and an affected individual from each family (Table 2), DNA was extracted from peripheral blood or amniocytes (QiaSymphony BioRobot, QIAGEN). One microgram of extracted DNA was sheared into 150–200 bp fragments that were ligated to adaptors and purified for subsequent polymerase chain reaction (PCR) amplification. Amplified products were subjected to capture by biotinylated RNA library baits in solution, according to the manufacturer's instructions. Bound DNA was isolated with streptavidin-coated beads and reamplified. The final products were sequenced with the Illumina HiSeq 2500 sequencing system with 100-bp paired-end reads (Illumina). Data were aligned to UCSC Genome Browser build hg19 by the Burroughs Wheeler Aligner.[20] Local realignment was performed with the Genome Analysis Toolkit Indel Realigner and variants were called with SAMtools. Variant calling was performed on probands and both parents. Variants were confirmed by Sanger sequencing with BigDye Terminator Cycle Sequencing Kit (Applied Biosystems) and AxyPrep Mag DyeClean Kit (Axygen Biosciences) on an Applied Biosystems 3730xl DNA Analyzer. Primer sequences are available upon request. To screen for *NPHS1* deletions and duplications, we used ExonArrayDx (GeneDx) that contains DNA oligonucleotide probes and is designed to detect most single-exon deletions and duplications, with probe sequences and locations based on Genome Reference Consortium build 37 (GRCh37)/UCSC hg19. Data analysis was performed with Agilent Genomic Workbench software, with gene-specific filtering by Cartagenia BENCH software. The model of CRB2 was computed with multitemplate MODELLER9.14 protocol.[21] The template structures (PDB codes 2wjs, 3qcw, 4d90, 2m74, 4d0e) were detected with HHpred.[22]

Table 2. Four Mutations in *CRB2* Described in this Report

Nucleotide Alteration	Amino Acid Alteration	SIFT	PolyPhen-2	Mutation Taster	NHLBI Exome Variant Server	Predicted Effect
c.1897C>T	p.Arg633Trp	0.002	PD[e]; 1.0	DC[f]; 0.994	not present	mutation
c.1928A>C	p.Glu643Ala	0.007	PD; 0.999	DC; 0.999	not present	mutation
c.2277G>A	p.Trp759Ter	–	–	DC; 1.0	1/6501	mutation
c.2400C>G	p.Asn800Lys	0.004	PD; 0.999	DC; 0.999	not present	mutation

Abbreviations are as follows: DC, disease causing; PD, probably damaging.

In the first family, exome sequencing performed on DNA extracted from amniocytes from the second affected fetus revealed compound heterozygosity for two deleterious sequence variants in *CRB2* (Transcript NM_173689.6): c.2277G>A, predicting a nonsense variant, p.Trp759Ter, that was paternally inherited, and c.2400C>G, predicting p.Asn800Lys, that was maternally inherited (Protein NP_775960.4; Table 2; Figure S1A available online). Both mutations were predicted to be disease causing (Mutation Taster) and the second was predicted to be probably damaging (PolyPhen-2; Table 2). Targeted sequencing of cultured skin fibroblasts from the first affected fetus also revealed the same *CRB2* mutations. The couple's healthy son was heterozygous for p.Trp759Ter and did not inherit the second mutation, consistent with autosomal-recessive inheritance.

In the second family, WES performed on the third affected fetus showed compound heterozygosity for two *CRB2* mutations: c.1928A>C, predicting p.Glu643Ala that was maternally inherited, and c.2400C>G, predicting p.Asn800Lys, that was paternally inherited (Table 2; Figure S1B). Both mutations were predicted to be disease causing (Mutation Taster) and probably damaging (PolyPhen-2; Table 2). No DNA was available from the first two affected fetuses. A healthy son and daughter, born to the same parents, did not inherit either mutation.

In the third family, homozygosity for c.1897C>T, predicting p.Arg633Trp in *CRB2*, was identified in the affected child and both parents were heterozygous (Table 2; Figure S1C). This mutation was predicted to be disease causing (Mutation Taster) and probably damaging (PolyPhen-2; Table 2). WES also showed a paternally inherited, splice site mutation, c.1440+1G>A in *NPHS1* (RefSeq NM_004646.3), that was predicted to destroy the canonical splice donor site in intron 11, resulting in an abnormal mRNA subject to nonsense-mediated decay or to an abnormal protein product. c.1440+1G>A was not observed in the NHLBI Exome Variant Server and was interpreted as a disease-causing mutation. Testing for *NPHS1* deletions and duplications was negative by targeted array CGH with exon-level resolution and a second mutation was not detected. Sequencing of the polycystin 1 (*PKD1* [MIM 601313]) and polycystin 2 (*PKD2* [MIM 173910]) genes revealed heterozygosity for c.10141A>G, predicting p.His3311Arg (RefSeq NM_00109944.2), in *PKD1* that was interpreted as a variant of unknown significance. A missense substitution, p.Asn327Ser, in sushi repeat containing protein, X-linked (*SRPX2* [MIM 300642]; RefSeq NM_014467.2) was also observed, but predicted to be benign (PolyPhen-2 score 0.063). In view of the similarity of the clinical findings in this child to the other cases with *CRB2* mutations, *CRB2* was considered to be the pathogenic gene.

We have described five fetuses and a male child with a rare, severe phenotype comprising brain malformations with marked cerebral ventriculomegaly, gray matter heterotopias, renal disease consistent with nephrosis with the presence of renal microcysts, and striking elevations of MSAFP and AFAFP (Table 1). The clinical findings could be attributed to autosomal-recessive inheritance of deleterious *CRB2* sequence variants in all affected fetuses and the affected child (Table 2). All pregnancies were abnormal, with ascertainment due to high AFP levels or US findings prior to the end of the second trimester and the cerebral ventriculomegaly was detectable from 16 weeks of gestation. Cardiac involvement was suggested by the VSD and mild aortic dilatation seen in one affected individual (Table 1) but has so far been infrequent. The gestation of the fetuses and early demise of the affected child prevented eye examination, and thus it is not known whether ocular findings similar to RP or LCA develop. Two families in this report carried the same mutation, p.Asn800Lys (Table 2). Both families shared Ashkenazi Jewish ethnicity and it is possible that this represents a founder mutation. Further analysis might reveal a common haplotype or increased frequency of this mutation in Ashkenazi Jewish individuals. Loss of function is suggested by the occurrence of one nonsense mutation, p.Trp759Ter.

The histopathological features of the kidneys in the third affected fetus from family 2 are similar to those observed in congenital nephrotic syndrome, Finnish type. Light microscopy findings in this syndrome include immature glomeruli with minimal glomerular changes, mesangial hypercellularity, and (in advanced cases) focal and global glomerulosclerosis. There is characteristic microcystic dilatation of proximal and distal tubules with protein reabsorption droplets. Electron microscopic studies show diffuse foot process effacement with absence of slit diaphragm and variable villous transformation.[23–25] This form of congenital nephrotic syndrome is an

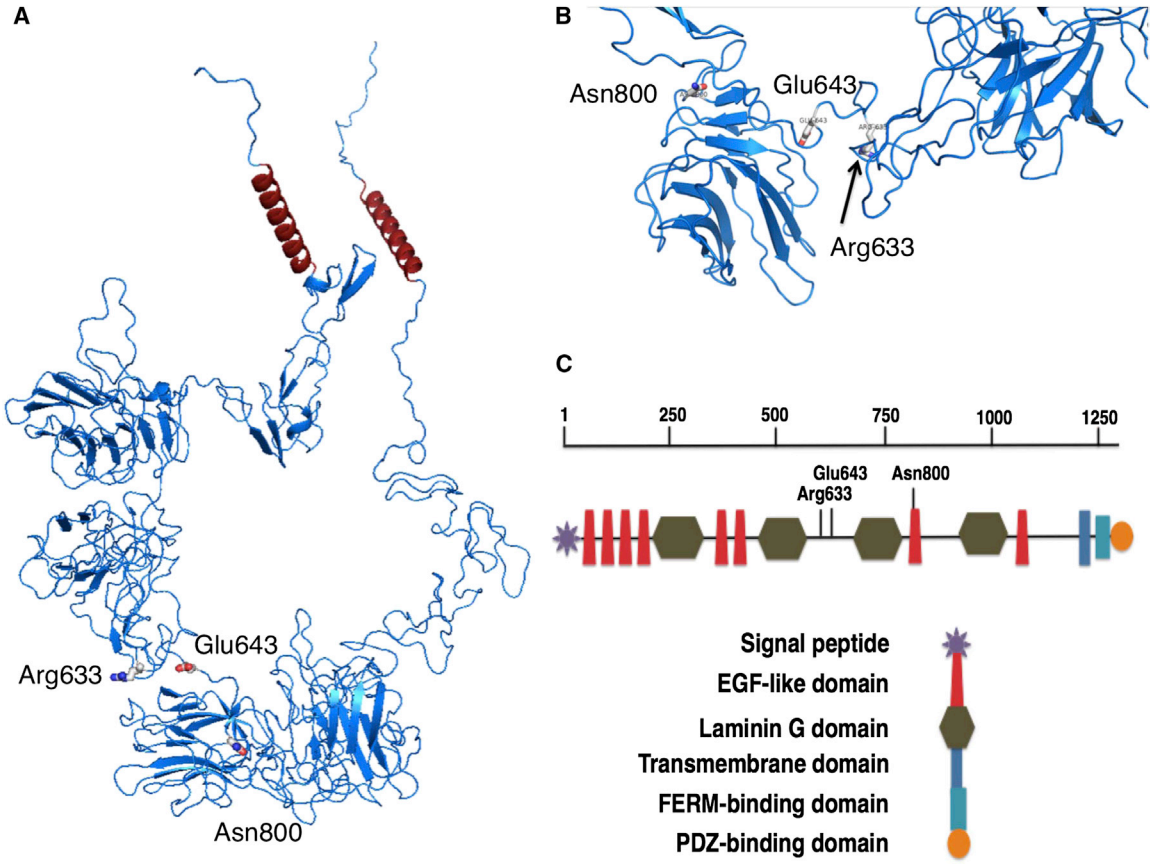

Figure 3. Position of Three Mutated Residues in CRB2
(A and B) Model of CRB2 showing mutation position for Arg633, Glu643, and Asn800. Arg633 and Glu643 are positioned between protein domains, whereas Asn800 is adjacent to an EGF-like domain.
(C) Schema showing approximate mutation position for Arg633, Glu643, and Asn800. CRB2 domains were defined according to the structure of the model and the National Center for Biotechnology Information Conserved Domains Database.

autosomal-recessive condition characterized by massive proteinuria at birth, significant elevations of AFP, a large placenta, and marked edema within the first months of life.[26] Microcystic dilatation of the proximal renal tubules is present from 18 to 20 weeks of gestation and there is complete effacement of the foot processes and swelling of endothelial cells in the glomerular capillary loops, leading to abnormal permeability and protein filtration.[26] The condition is caused by mutations in *NPHS1*, which encodes nephrin, a protein that is present in the slit-diaphragm spanning the distal foot process and which functions a tight junction for ultrafiltration in the podocytes that surround the vascular region of the glomerulus.[27–29] The histopathological and ultrastructural features observed are not specific to Finnish nephropathy and can also be seen in podocin deficiency (MIM 600995), which accounts for 15% of nephrotic syndrome in the first 3 months of life and is caused by mutations in *NPHS2* (MIM 604766).[30,31]

The strong overlap between the renal phenotypes observed in the families reported and those with congenital nephrosis spectrum suggests common pathophysiology between the two conditions. Similarities in phenotype have also been found in animal models of loss of *crb2* or *nphs1* function. There are two *crb2* orthologs in *Danio rerio*, and *crb2b* is expressed in the pronephric glomerulus from 48 hr postfertilization (hpf) until 96 hpf at the time of podocyte differentiation.[28] In *Danio rerio* injected with antisense morpholinos targeting *crb2b*, compromise of glomerular permeability and cardiac edema with pronephric cysts was observed. Histology of the morphants showed abnormal glomerular histology, with an expanded Bowman's space, disorganization of the podocyte foot process architecture, and a loss of slit diaphragms.[28] In *Danio rerio* with loss of nephrin, a similar but milder phenotype was observed, with loss of the slit diaphragms but preservation of the foot processes.[28,32]

Models of CRB2 have shown that the majority of the protein is extracellular, with a short cytoplasmic segment containing the PDZ-binding domains that interacts with Protein Associated with Lin7 1 (PALS1)/Membrane protein, palmitoylated 5 (MPP5 [MIM 606958]).[33] The three missense mutations described in these families affect residues from the extracellular region of CRB2 (Figure 3), and thus it is unlikely that they disturb formation of the Crumbs complex and affect cell polarity. The finding that the human mutations are unlikely to impair apical-basal polarity is consistent with studies in *Danio rerio*, which

showed that antisense morpholinos targeting *crb2b* do not disturb the overall polarity of podocytes, which continue to contact the glomerular basement membrane.[28] In the morpholino studies, nephrin was apically mistargeted in the podocytes, and it is possible that this mislocalization prevented normal maturation of the slit diaphragm.[28] However, because nephrin is primarily an extracellular protein, it is also plausible that both proteins are required for cell-cell interactions or cell-matrix interactions that ensure tight cellular contact.

It is unclear whether the same mechanism underlying the renal defects associated with *CRB2* loss of function is also responsible for the cerebral malformations. In *Danio rerio*, *crb2a* and *crb2b* are expressed in the apical surface of the optic vesicle and the neuroepithelium of the ventral diencephalon at the 10 somite stage, although antisense morpholino studies targeting *crb1*, *crb2a*, and *crb2b* suggested that these genes have functional redundancy in maintaining apicobasal polarity of the neuroepithelium.[34] Interestingly, mice that are homozygous null for Lethal giant larvae 1 (*Lgl1* [MIM 600966]), a gene implicated the maintenance of cell polarity in *Drosophila*, develop severe hydrocephalus that is lethal in the neonatal period.[35] Because the human mutations are not predicted to disrupt polarity, the significance of these studies to CRB2 is uncertain.

We were able to find only a few earlier reports in which congenital nephrotic syndrome has been associated with cerebral ventriculomegaly, and the lack of molecular information in these previous cases prevents firm conclusions. In one family, the father had six affected children, four with a first cousin, and two with a second cousin.[36] Clinical findings among the cases included ventriculomegaly with dilatation of the lateral ventricles and focal hyperplasia of the choroid plexus. The kidneys were normal in size but were echodense, and there were multiple small cysts in the corticomedullary area and in the renal medulla that contained amorphous, proteinaceous material. Five fetuses had markedly elevated AFP levels and AF was positive for acetylcholinesterase. Karyotypes were normal in all cases examined and one fetus had a large placenta that comprised 25% of fetal weight.[36] Lastly, a strikingly similar phenotype with raised MSAFP and AFAFP levels, ventriculomegaly, renal hyperechogenicity and cysts, and cardiac involvement with dilatation of the right heart and pericardial effusion has been reported (Table S1).[37] One fetus had an absent horizontal fissure of the right lung, incomplete rotation of the intestine, and a small thymus, spleen, and adrenal glands. Similarities with the cases in this report also include mention of reduced kidney weight at autopsy.[37]

In summary, the three families with six affected individuals present compelling evidence for the role of *CRB2* in human disease, with a phenotype comprising severe, congenital neurological and renal involvement. The clinical features and pathophysiology resemble congenital nephrotic syndrome, Finnish type, with significantly elevated MSAFP or AFAFP measurements, renal microcysts, and effacement of the podocyte foot processes, and thus mutations in *CRB2* should be considered in the differential diagnosis of this condition.

Supplemental Data

Supplemental Data include one figure and one table and can be found with this article online at http://dx.doi.org/10.1016/j.ajhg.2014.11.013.

Acknowledgments

We are very grateful to the families for their participation. We are also very thankful to Dr. James Barkovich for his help with the analysis of the MRI scans. S.J.D. is an employee of GeneDx and H.P. was previously an employee of GeneDx.

Received: October 8, 2014
Accepted: November 21, 2014
Published: December 31, 2014

Web Resources

The URLs for data presented herein are as follows:

Burrows-Wheeler Aligner, http://bio-bwa.sourceforge.net/
MutationTaster, http://www.mutationtaster.org/
NCBI Conserved Domains, http://www.ncbi.nlm.nih.gov/Structure/cdd/wrpsb.cgi
NHLBI Exome Sequencing Project (ESP) Exome Variant Server, http://evs.gs.washington.edu/EVS/
Online Mendelian Inheritance in Man (OMIM), http://www.omim.org/
PolyPhen-2, http://www.genetics.bwh.harvard.edu/pph2/
SAMtools, http://samtools.sourceforge.net/
SIFT, http://sift.bii.a-star.edu.sg/

References

1. Gosens, I., den Hollander, A.I., Cremers, F.P., and Roepman, R. (2008). Composition and function of the Crumbs protein complex in the mammalian retina. Exp. Eye Res. *86*, 713–726.
2. Tepass, U., Theres, C., and Knust, E. (1990). crumbs encodes an EGF-like protein expressed on apical membranes of *Drosophila* epithelial cells and required for organization of epithelia. Cell *61*, 787–799.
3. Tepass, U., and Knust, E. (1993). Crumbs and stardust act in a genetic pathway that controls the organization of epithelia in *Drosophila melanogaster*. Dev. Biol. *159*, 311–326.
4. Tanentzapf, G., and Tepass, U. (2003). Interactions between the crumbs, lethal giant larvae and bazooka pathways in epithelial polarization. Nat. Cell Biol. *5*, 46–52.
5. Katoh, M., and Katoh, M. (2004). Identification and characterization of Crumbs homolog 2 gene at human chromosome 9q33.3. Int. J. Oncol. *24*, 743–749.
6. Pocha, S.M., and Knust, E. (2013). Complexities of Crumbs function and regulation in tissue morphogenesis. Curr. Biol. *23*, R289–R293.
7. Alves, C.H., Sanz, A.S., Park, B., Pellissier, L.P., Tanimoto, N., Beck, S.C., Huber, G., Murtaza, M., Richard, F., Sridevi Gurubaran, I., et al. (2013). Loss of CRB2 in the mouse retina

mimics human retinitis pigmentosa due to mutations in the CRB1 gene. Hum. Mol. Genet. *22*, 35–50.
8. Chen, C.L., Gajewski, K.M., Hamaratoglu, F., Bossuyt, W., Sansores-Garcia, L., Tao, C., and Halder, G. (2010). The apical-basal cell polarity determinant Crumbs regulates Hippo signaling in *Drosophila*. Proc. Natl. Acad. Sci. USA *107*, 15810–15815.
9. Pellissier, L.P., Alves, C.H., Quinn, P.M., Vos, R.M., Tanimoto, N., Lundvig, D.M., Dudok, J.J., Hooibrink, B., Richard, F., Beck, S.C., et al. (2013). Targeted ablation of CRB1 and CRB2 in retinal progenitor cells mimics Leber congenital amaurosis. PLoS Genet. *9*, e1003976.
10. Alves, C.H., Pellissier, L.P., Vos, R.M., Garcia Garrido, M., Sothilingam, V., Seide, C., Beck, S.C., Klooster, J., Furukawa, T., Flannery, J.G., et al. (2014). Targeted ablation of Crb2 in photoreceptor cells induces retinitis pigmentosa. Hum. Mol. Genet. *23*, 3384–3401.
11. Jacobson, S.G., Cideciyan, A.V., Aleman, T.S., Pianta, M.J., Sumaroka, A., Schwartz, S.B., Smilko, E.E., Milam, A.H., Sheffield, V.C., and Stone, E.M. (2003). Crumbs homolog 1 (CRB1) mutations result in a thick human retina with abnormal lamination. Hum. Mol. Genet. *12*, 1073–1078.
12. den Hollander, A.I., Davis, J., van der Velde-Visser, S.D., Zonneveld, M.N., Pierrottet, C.O., Koenekoop, R.K., Kellner, U., van den Born, L.I., Heckenlively, J.R., Hoyng, C.B., et al. (2004). CRB1 mutation spectrum in inherited retinal dystrophies. Hum. Mutat. *24*, 355–369.
13. Tiab, L., Largueche, L., Chouchane, I., Derouiche, K., Munier, F.L., El Matri, L., and Schorderet, D.F. (2013). A novel homozygous R764H mutation in crumbs homolog 1 causes autosomal recessive retinitis pigmentosa. Mol. Vis. *19*, 829–834.
14. Khan, A.O., Aldahmesh, M.A., Abu-Safieh, L., and Alkuraya, F.S. (2014). Childhood cone-rod dystrophy with macular cystic degeneration from recessive CRB1 mutation. Ophthalmic Genet. *35*, 130–137.
15. Tsang, S.H., Burke, T., Oll, M., Yzer, S., Lee, W., Xie, Y.A., and Allikmets, R. (2014). Whole exome sequencing identifies CRB1 defect in an unusual maculopathy phenotype. Ophthalmology *121*, 1773–1782.
16. Roh, M.H., Makarova, O., Liu, C.J., Shin, K., Lee, S., Laurinec, S., Goyal, M., Wiggins, R., and Margolis, B. (2002). The Maguk protein, Pals1, functions as an adapter, linking mammalian homologues of Crumbs and Discs Lost. J. Cell Biol. *157*, 161–172.
17. Watanabe, T., Miyatani, S., Katoh, I., Kobayashi, S., and Ikawa, Y. (2004). Expression of a novel secretory form (Crb1s) of mouse Crumbs homologue Crb1 in skin development. Biochem. Biophys. Res. Commun. *313*, 263–270.
18. van den Hurk, J.A., Rashbass, P., Roepman, R., Davis, J., Voesenek, K.E., Arends, M.L., Zonneveld, M.N., van Roekel, M.H., Cameron, K., Rohrschneider, K., et al. (2005). Characterization of the Crumbs homolog 2 (CRB2) gene and analysis of its role in retinitis pigmentosa and Leber congenital amaurosis. Mol. Vis. *11*, 263–273.
19. Xiao, Z., Patrakka, J., Nukui, M., Chi, L., Niu, D., Betsholtz, C., Pikkarainen, T., Vainio, S., and Tryggvason, K. (2011). Deficiency in Crumbs homolog 2 (Crb2) affects gastrulation and results in embryonic lethality in mice. Dev. Dyn. *240*, 2646–2656.
20. Li, H., and Durbin, R. (2009). Fast and accurate short read alignment with Burrows-Wheeler transform. Bioinformatics *25*, 1754–1760.
21. Sali, A., and Blundell, T.L. (1993). Comparative protein modelling by satisfaction of spatial restraints. J. Mol. Biol. *234*, 779–815.
22. Söding, J. (2005). Protein homology detection by HMM-HMM comparison. Bioinformatics *21*, 951–960.
23. Liapis, H. (2008). Molecular pathology of nephrotic syndrome in childhood: a contemporary approach to diagnosis. Pediatr. Dev. Pathol. *11*, 154–163.
24. Machuca, E., Benoit, G., and Antignac, C. (2009). Genetics of nephrotic syndrome: connecting molecular genetics to podocyte physiology. Hum. Mol. Genet. *18* (R2), R185–R194.
25. Santín, S., García-Maset, R., Ruíz, P., Giménez, I., Zamora, I., Peña, A., Madrid, A., Camacho, J.A., Fraga, G., Sánchez-Moreno, A., et al.; FSGS Spanish Study Group (2009). Nephrin mutations cause childhood- and adult-onset focal segmental glomerulosclerosis. Kidney Int. *76*, 1268–1276.
26. Machuca, E., Benoit, G., Nevo, F., Tête, M.J., Gribouval, O., Pawtowski, A., Brandström, P., Loirat, C., Niaudet, P., Gubler, M.C., and Antignac, C. (2010). Genotype-phenotype correlations in non-Finnish congenital nephrotic syndrome. J. Am. Soc. Nephrol. *21*, 1209–1217.
27. Pavenstädt, H., Kriz, W., and Kretzler, M. (2003). Cell biology of the glomerular podocyte. Physiol. Rev. *83*, 253–307.
28. Ebarasi, L., He, L., Hultenby, K., Takemoto, M., Betsholtz, C., Tryggvason, K., and Majumdar, A. (2009). A reverse genetic screen in the zebrafish identifies crb2b as a regulator of the glomerular filtration barrier. Dev. Biol. *334*, 1–9.
29. Ichimura, K., Fukuyo, Y., Nakamura, T., Powell, R., Sakai, T., and Obara, T. (2012). Structural disorganization of pronephric glomerulus in zebrafish mpp5a/nagie oko mutant. Dev. Dyn. *241*, 1922–1932.
30. Hinkes, B.G., Mucha, B., Vlangos, C.N., Gbadegesin, R., Liu, J., Hasselbacher, K., Hangan, D., Ozaltin, F., Zenker, M., and Hildebrandt, F.; Arbeitsgemeinschaft für Paediatrische Nephrologie Study Group (2007). Nephrotic syndrome in the first year of life: two thirds of cases are caused by mutations in 4 genes (NPHS1, NPHS2, WT1, and LAMB2). Pediatrics *119*, e907–e919.
31. Philippe, A., Nevo, F., Esquivel, E.L., Reklaityte, D., Gribouval, O., Tête, M.J., Loirat, C., Dantal, J., Fischbach, M., Pouteil-Noble, C., et al. (2008). Nephrin mutations can cause childhood-onset steroid-resistant nephrotic syndrome. J. Am. Soc. Nephrol. *19*, 1871–1878.
32. Fukuyo, Y., Nakamura, T., Bubenshchikova, E., Powell, R., Tsuji, T., Janknecht, R., and Obara, T. (2014). Nephrin and Podocin functions are highly conserved between the zebrafish pronephros and mammalian metanephros. Mol. Med. Rep. *9*, 457–465.
33. Pieczynski, J., and Margolis, B. (2011). Protein complexes that control renal epithelial polarity. Am. J. Physiol. Renal Physiol. *300*, F589–F601.
34. Zou, J., Wen, Y., Yang, X., and Wei, X. (2013). Spatial-temporal expressions of Crumbs and Nagie oko and their interdependence in zebrafish central nervous system during early development. Int. J. Dev. Neurosci. *31*, 770–782.
35. Klezovitch, O., Fernandez, T.E., Tapscott, S.J., and Vasioukhin, V. (2004). Loss of cell polarity causes severe brain dysplasia in Lgl1 knockout mice. Genes Dev. *18*, 559–571.
36. Reuss, A., den Hollander, J.C., Niermeijer, M.F., Wladimiroff, J.W., van Diggelen, O.P., Lindhout, D., and Los, F.J. (1989). Prenatal diagnosis of cystic kidney disease with ventriculomegaly: a report of six cases in two related sibships. Am. J. Med. Genet. *33*, 385–389.
37. Jolly, M., Goodburn, S., Cox, P., and Loughna, P. (2003). Congenital nephropathy and ventriculomegaly: a report of four cases. Prenat. Diagn. *23*, 48–51.